

Original Article

# Reassessment of subacute MPTP-treated mice as animal model of Parkinson's disease

Qiu-shuang ZHANG<sup>1</sup>, Yang HENG<sup>1</sup>, Zheng MOU<sup>1</sup>, Ju-yang HUANG<sup>1</sup>, Yu-he YUAN<sup>1, \*</sup>, Nai-hong CHEN<sup>1, 2, \*</sup>

<sup>1</sup>State Key Laboratory of Bioactive Substances and Functions of Natural Medicines, Institute of Materia Medica & Neuroscience Center, Chinese Academy of Medical Sciences and Peking Union Medical College, Beijing 100050, China; <sup>2</sup>College of Pharmacy, Hunan University of Chinese Medicine, Changsha 410208, China

## Abstract

1-Methyl-4-phenyl-1,2,3,6-tetrahydropyridine (MPTP) mouse model remains the most commonly used animal model of Parkinson's disease (PD). There are three MPTP-treatment schemes: acute, subacute and chronic. Considering the advantages of the period and similarity to PD, the subacute model was often chosen to assess the validity of new candidates, but the changes caused by the subacute MPTP treatment and the appropriate positive control for this model remain to be further confirmed. The aim of this study was: to estimate the value of the subacute MPTP mouse model in aspects of behavioral performance, biochemical changes and pathological abnormalities, and to find effective positive drugs. Male C57BL/6 mice were injected with MPTP (30 mg·kg<sup>-1</sup>·d<sup>-1</sup>, ip) for 5 consecutive days. Three days before MPTP injection, the mice were orally administered selegiline (3 mg·kg<sup>-1</sup>·d<sup>-1</sup>), pramipexole (3 mg·kg<sup>-1</sup>·d<sup>-1</sup>), or medopar (100 mg·kg<sup>-1</sup>·d<sup>-1</sup>) for 18 days. Behavioral performance was assessed in the open field test, pole test and rotarod test. Neurotransmitters in the striatum were detected using HPLC. Protein levels were measured by Western blot. Pathological characteristics were examined by immunohistochemistry. Ultrastructure changes were observed by electron microscopy. The subacute MPTP treatment did not induce evident motor defects despite severe injuries in the dopaminergic system. Additionally, MPTP significantly increased the  $\alpha$ -synuclein levels and the number of astrocytes in the striatum, and destroyed the blood-brain barrier (BBB) in the substantia nigra pars compacta. Both selegiline and pramipexole were able to protect the mice against MPTP injuries. We conclude that the subacute MPTP mouse model does not show visible motor defects; it is not enough to evaluate the validity of a candidate just based on behavioral examination, much attention should also be paid to the alterations in neurotransmitters, astrocytes,  $\alpha$ -synuclein and the BBB. In addition, selegiline or pramipexole is a better choice than medopar as an effective positive control for the subacute MPTP model.

**Keywords:** Parkinson's disease; MPTP model; selegiline; pramipexole; medopar; behavioral compensation; astrocytes;  $\alpha$ -synuclein; blood brain barrier; myelin sheath

Acta Pharmacologica Sinica (2017) 38: 1317–1328; doi: 10.1038/aps.2017.49; published online 26 Jun 2017

## Introduction

Parkinson's disease (PD), the second most common neurodegenerative disease, affects over 1% of the population above 60 years old<sup>[1]</sup>. Clinically, PD patients suffer low quality of life with motor disorders such as resting tremor, muscle rigidity, bradykinesia, and postural instability<sup>[2]</sup>. The pathological characteristics of PD include progressive destruction of the nigrostriatal system, formulation of Lewy bodies (LBs), and sustaining inflammation<sup>[3]</sup>. Up until now, PD remains incurable, and the primary therapy relies on medications<sup>[4]</sup> such

as L-dopa (usually combined with a peripheral dopa decarboxylase inhibitor), dopamine receptor agonists, monoamine oxidase B (MAO-B) inhibitors, central anticholinergic agents, neuroprotective agents, or amantadine. However, all of these medicines mainly improve motor symptoms but fail to prevent the degeneration associated with PD<sup>[4]</sup>. Therefore, the development of new medications to halt or reverse the progress of PD is important. Until recently, many models based on etiology, such as neurotoxin models and transgenic models<sup>[5]</sup>, have been used to research PD pathogenesis or effective treatment compounds. Among all of these models, the MPTP mouse model remains the most commonly used animal model of PD.

There are three MPTP-treatment schemes<sup>[6–9]</sup>: acute, subacute, and chronic. Considering the advantages of the period and

\*To whom correspondence should be addressed.

E-mail yuanyuhe@imm.ac.cn (Yu-he YUAN);

chennh@imm.ac.cn (Nai-hong CHEN)

Received 2016-12-29 Accepted 2017-03-30

similarity to PD, researchers often choose the subacute model to assess the validity of some candidates, but the changes caused by the subacute MPTP treatment and the appropriate positive control for this model still need to be further confirmed.

Therefore, in this work, MPTP-treated mice were treated with three types of medications for PD (selegiline, pramipexol, medopar) to confirm the value of this model and an effective drug to treat it.

## Materials and methods

### Animals and reagents

Male C57BL/6 mice (8 weeks, 22–25 g), purchased from Vital River (Charles River Co, Beijing, China), were used for experiments. All mice were raised in an environment with a 12-h light/dark cycle at a temperature of  $22\pm 1$  °C with available food and water. All experiments were conducted according to the principles established for the care and use of laboratory animals by the National Institutes of Health and were approved by the Animal Care Committee of the Chinese Academy of Medical Sciences. Tablets of selegiline hydrochloride (Orion Co, Finland), pramipexol hydrochloride (Boehringer Ingelheim Pharma GmbH & Co KG, Germany), and medopar (Roche Pharmaceuticals Ltd, Shanghai, China) were purchased from Beijing Hospital. MPTP hydrochloride was obtained from Sigma Corporation (Sigma-Aldrich, St Louis, MO, USA).

### Experimental procedures

Experimental procedures (Figure 1A) were conducted as follows. After mice adapted for one week and were trained for the behavioral tests, they were divided into five groups randomly (Figure 1B): the control group (equal volume of water), the model group (equal volume of water), the selegiline group (3 mg/kg), the pramipexole group (3 mg/kg), and the medopar group (100 mg/kg). Three days before MPTP treatment, mice were given the drug treatment or an equal volume of water intragastrically for 18 days. To construct the model, mice were injected with MPTP (dissolved in 0.9% saline, 30 mg/kg, ip) for 5 consecutive days, while the control group was given an equal volume of normal saline (ip). Two days after the last injection, behavioral assessments were performed using the open field test, pole test and rotarod test. On the 19th day, all animals were sacrificed for further study.

### Open field test

The method was modified from the reported protocol<sup>[10]</sup>. A white opaque plastic box (48 cm×32 cm×20 cm) was used for the open field. The floor of the box was divided into 24 grids of 8 cm×8 cm. Before estimation, all mice were pre-adapted to the box for 5 min. The next day, the mouse was placed in the center of the open field and video recorded for 5 min. The box was cleaned with 10% alcohol and water between trials. Then, the distance traveled and the amount of rearing in 5 min were manually scored.

### Rotarod test

Mouse motor coordination was evaluated by using a rotarod

apparatus (IITC Life Science, CA, USA) as described previously<sup>[11]</sup>. Before administration, all mice were trained on the rotarod (5 to 10 r/min in 300 s linearly) for 300 s. This training process was performed for more than 3 rounds to train all mice to walk on the rotarod. After MPTP treatment, the rotarod test was conducted at a uniformly accelerating speed from 5 to 30 r/min in 300 s, and the latency to fall was recorded.

### Pole test

The pole test was implemented as described in our previous work<sup>[11]</sup> to evaluate the movement disorder of the mice. The apparatus consisted of a wooden pole (50 cm high, 0.5 cm in diameter, wrapped with gauze to prevent slipping) with a wooden ball at the top. The base of the pole was covered with bedding as a protection for mice from injury. After acclimatization, the mice were pre-trained with the pole three times to make sure that all animals would turn head down once they were put on the ball. During the pole test, the total time it took for the mouse to get from the top to the bottom was measured.

### Tissue preparation

Mice were anesthetized with chloral hydrate (400 mg/kg, ip). The striatum was rapidly dissected, frozen in dry ice and stored at -80 °C for biochemical analysis. For histological analysis, mice were anesthetized and perfused with 0.1 mol/L phosphate-buffered saline (PBS), followed by 4% paraformaldehyde (PFA). Later, the mouse brains were collected and post-fixed in 4% PFA for 24 h. After fixation, the brains were dehydrated with different concentrations of sucrose (from 10%, 20%, finally to 30%) until the brain samples were at the bottom of the solution. Then, coronal sections (20 μm thick) containing the striatum or substantia nigra pars compacta (SNpc) were cut on a cryostat (CM3050S, Leica, Germany) and placed on coated slides for analysis.

### Electron microscopic analysis

Briefly, following perfusion, cubes (1 mm<sup>3</sup>) of SNpc or the lumbar spinal anterior horn were successively treated as follows: fixed in 2.5% glutaraldehyde, cut into ultrathin sections, stained with uranyl acetate and lead citrate, and then finally imaged by transmission electron microscopy (TEM) (H-7650, HITACHI, Japan) for ultrastructure analysis.

### Immunohistochemistry

The slices of striatum or SN were treated as follows: boiled in 0.01 mol/L citrate buffer solution for 10 min to retrieve antigen, steeped in 1% Triton X-100 for 10 min to increase the penetration of the antibody, incubated with 3% hydrogen peroxide (H<sub>2</sub>O<sub>2</sub>) for 10 min to eliminate endogenous peroxidase activity, and incubated in 5% bovine serum albumin (BSA) for 1 h to remove the non-specific binding. Additionally, these slices were washed with PBST (5 min once, 3 times) between every two steps. Then, they were incubated with primary antibodies, including anti-tyrosine hydroxylase (TH) (1:100, Santa Cruz, Dallas, TX, USA), anti-α-synuclein (1:100,

Abcam, Cambridge, CB, UK), and anti-gial fibrillary acidic protein (GFAP) (1:500, Dako, Denmark), overnight at 4 °C. After washing, slices were incubated with the corresponding horseradish peroxidase-conjugated secondary antibodies (1:200, KPL, Gaithersburg, MD, USA) for 2 h and washed three times. Then, the slices were stained with 3,3'-diaminobenzidine (DAB) for 10–60 s and finally imaged with an Olympus BA51 photomicroscope (Tokyo, Japan). For TH<sup>+</sup> cell analysis, Image-Pro Plus 6.0 software (MediaCybernetics, USA) was used to calculate the total area of all cells in the SNpc region at 100× magnification. We ensured that the regions of interest among the different groups shared the same SN shape, and three slices of each group were needed for statistical analysis. Similarly, GFAP<sup>+</sup> cells were counted at 200× magnification in the same region of the striatum using Image-Pro Plus 6.0 software.

#### High-performance liquid chromatography (HPLC)

Striatum tissue samples were homogenized (1 mg: 10 mL, ice cold) in solution A (0.6 mol/L HClO<sub>4</sub>, and 375 ng/ml isoprenaline) and centrifuged (20000×g, 4 °C) for 20 min. The supernatant was collected and mixed with a half-volume of solution B (20 mmol/L potassium citrate, 300 mmol/L K<sub>2</sub>HPO<sub>4</sub>, and 2 mmol/L EDTA-2Na). After the samples were placed on ice for 30 min and centrifuged (20000×g, 4 °C) for 20 min, the supernatant was analyzed using the HPLC system (Waters e2695, USA). The mobile phase (100 mmol/L sodium acetate anhydrous, 85 mmol/L citric acid, 0.5 mmol/L 1-octanesulfonic acid sodium, 0.2 mmol/L EDTA-2Na, 15% methanol, pH=3.68) flowed at a rate of 1 mL/min. The electrochemical potential was at 760 mV compared with the reference electrode (Ag/AgCl), and the sensitivity was set at a full scale of 50 nA.

#### Western blot analysis

Brain tissue was diluted 20-fold (μL/mg) with ice-cold RIPA buffer (50 mmol/L Tris-HCl, pH 7.5, 150 mmol/L NaCl, 1 mmol/L EDTA, 0.5% sodium deoxycholate, 1% NP-40, 0.1% SDS, 0.1 mmol/L PMSF and 1% protease inhibitor cocktail) and disrupted on ice by using an ultrasonication apparatus (VTX 130, Sonics, USA). After the crushed tissue was lysed on ice for 30 min, it was centrifuged (12000×g, 4 °C) for 30 min. Then, the supernatants were collected, and the protein concentration was measured with a BCA kit. The extracted protein was denatured after it was boiled with loading buffer for 10 min. Protein samples of the same amount were separated by 15% SDS-PAGE gels and transferred to PVDF membranes (Millipore, USA). These membranes were blocked with 3% BSA (Sigma-Aldrich, St Louis, MO, USA) and incubated with primary antibodies such as anti-β-actin (1:5000, Sigma-Aldrich, St Louis, MO, USA), anti-TH (1:500, Santa Cruz, Dallas, TX, USA), anti-GFAP (1:500, Santa Cruz, Dallas, TX, USA), or anti-α-synuclein (1:500, Santa Cruz, Dallas, TX, USA), overnight at 4 °C. After the membranes were washed (10 min, 3 times), they were incubated with horseradish peroxidase-conjugated secondary antibody (1:5000, KPL, Gaithersburg, MD, USA) for

2 h. Protein bands were detected with an enhanced chemiluminescence (ECL) plus detection system (Molecular Device, Lmax). Finally, the intensity of each protein band was quantified by using image analysis software (Quantity One, Japan).

#### Statistical analysis

All results were statistically analyzed by ANOVA followed by Duncan's test or paired *t*-test. All data were expressed as the mean±SEM, and *P*<0.05 was considered to be significantly different.

## Results

### Body weight and movement performance

MPTP treatment showed no significant impact on mouse weight (Figure 1C). Additionally, the model mice failed to display motor impairments in the open field test (Figure 1D, 1E). Instead of a motor deficit, the rotarod test, however, showed that MPTP-treated mice exhibited a longer latency period (*P*<0.05) than the control group (Figure 1F). In addition, the pole test results showed that MPTP treatment did not significantly induce bradykinesia in mice (Figure 1G).

### Alteration of neurotransmitters in the striatum region

Neurotransmitters such as dopamine (DA), dihydroxyphenyl acetic acid (DOPAC), homovanillic acid (HVA), norepinephrine (NE) and serotonin (5-HT) in the striatum were detected by HPLC (Figure 2). First, the content of DA (*P*<0.01), DOPAC (*P*<0.01), and HVA in the striatum of the MPTP-injected group decreased significantly. Both selegiline (*P*<0.01 for DA and DOPAC) and pramipexole (*P*<0.01) attenuated these reductions, while medopar showed no effect. In addition, MPTP treatment markedly increased the ratios of DOPAC/DA (*P*<0.01) and HVA/DA (*P*<0.01), and selegiline administration significantly eliminated these changes (*P*<0.01). Furthermore, MPTP treatment significantly increased NE content (*P*<0.01), and selegiline (*P*<0.01), pramipexole (*P*<0.01) and medopar (*P*<0.01) significantly attenuated this change. What is more, MPTP injection decreased the striatal 5-HT level, and both selegiline (*P*<0.01) and pramipexole (*P*<0.05) alleviated this change, while medopar (*P*<0.05) led to a deeper decline.

### MPTP induced astrocyte activation and an increase in α-synuclein in the striatum region

Immunohistochemical staining showed that astrocytes in the striatum of the MPTP group were significantly activated and were inhibited after selegiline (*P*<0.01) and pramipexole administration (*P*<0.01) (Figure 3A, 3B). Meanwhile, the Western blot results showed the same trend (Figure 3C) with a significant increase in GFAP protein expression in the striatum after MPTP exposure (*P*<0.05) that was alleviated after selegiline or pramipexole administration. α-Synuclein is an important protein associated with PD. The immunohistochemical results suggested that MPTP treatment could increase the α-synuclein level in the striatum, which would be decreased by selegiline, pramipexole and medopar (Figure 3D), and the Western blot results demonstrated a similar trend (Figure 3E, 3F).

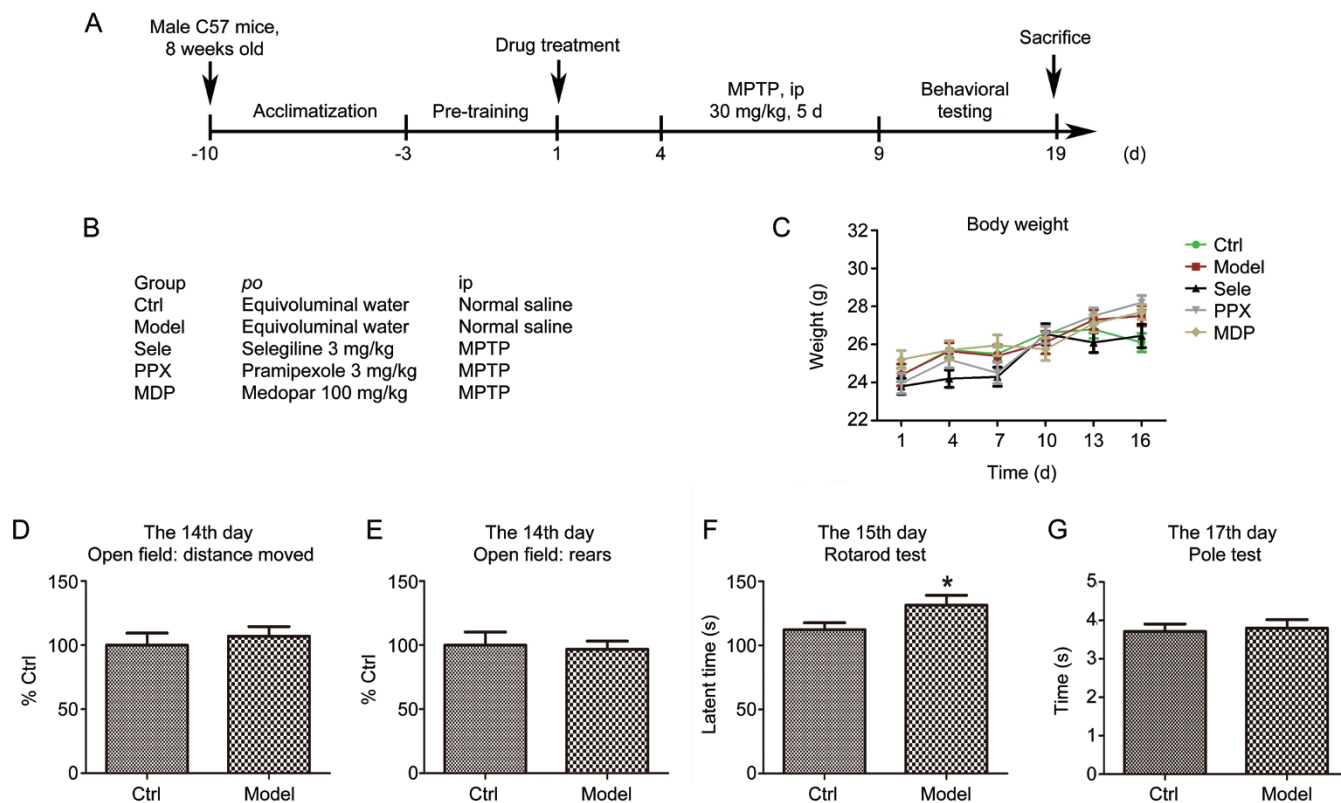


**Figure 1.** Experimental procedure, body weight and behavioral tests. (A, B) Experimental procedure and different drug administration schemes. (C) Body weight among groups showed no significant difference. (D–G) MPTP-treated mice displayed no motor impairment in the open field, exhibited a longer latency period in the rotarod test, and showed no deficits in the pole test. Data are presented as the mean  $\pm$  SEM.  $n > 10$ . One-way ANOVA test followed by Duncan's test or paired  $t$  test. \* $P < 0.05$  vs the control group.

### MPTP treatment led to damage of the nigrostriatal dopaminergic system

As the rate-limiting enzyme of DA synthesis, tyrosine hydroxylase (TH) is the biomarker of dopaminergic neurons. The immunohistochemical results for both TH-positive cell terminals in the striatum and TH-positive cell bodies in the SNpc revealed a severe dopaminergic neuron loss after MPTP exposure. Both selegiline and pramipexole protected these neurons against MPTP damage, while medopar did not show a protective function (Figure 4A). Furthermore, the Western blot results demonstrated that the striatal TH protein level of the model group was decreased by 40% compared with that of the control group ( $P < 0.01$ ), and selegiline ( $P < 0.01$ ) or pramipexole ( $P < 0.05$ ) but not medopar significantly attenuated this decrease (Figure 4B). Cell counting showed that the number of TH-positive cells in the SNpc of model mice decreased significantly ( $P < 0.01$ ) (Figure 4C), and selegiline ( $P < 0.01$ ) and pramipexole ( $P < 0.05$ ) significantly reduced this loss.

### MPTP treatment caused ultrastructure destruction in the SNpc region

In terms of the severe loss of dopaminergic neurons, further study in the SNpc region was performed through ultrastructure analysis (Figure 5). For a normal neuron, the nucleus is bright and round (Figure 5a), the nuclear chromatin is

dispersed evenly with low electron density (Figure 5a), and the organelles remain intact (Figure 5f). After exposure to MPTP, the neurons in the SNpc were damaged as follows: the nucleus shrank out of shape (Figure 5b); the chromatin was marked with heavy electron density and gathered near the outer nuclear layer (Figure 5b); the mitochondria and Golgi apparatus were swollen and incomplete (Figure 5g). These ultrastructural damages were improved after treatment with selegiline (Figure 5c, 5h) or pramipexole (Figure 5d, 5i). In addition, the blood vessels in the brain are wrapped by astrocyte endfeet to form the blood-brain barrier (BBB). The TEM images showed that the astrocyte endfeet were swollen after MPTP treatment, and therewith, the BBB was ruined (Figure 5l). The damaged BBB was ameliorated by selegiline (Figure 5m), pramipexole (Figure 5n) and medopar (Figure 5o) administration.

### MPTP induced ultrastructure destruction in the spinal cord

The spinal cord is responsible for delivering messages between the brain and the periphery. TEM images showed that (Figure 6) the myelin sheaths in the spinal cord of the normal mouse were organized regularly (Figure 6a), but following MPTP treatment, they were presented as discrete, loose, and out of order (Figure 6b). Except for the myelin sheaths, neurons in the spinal cord were also injured and featured as concentrated



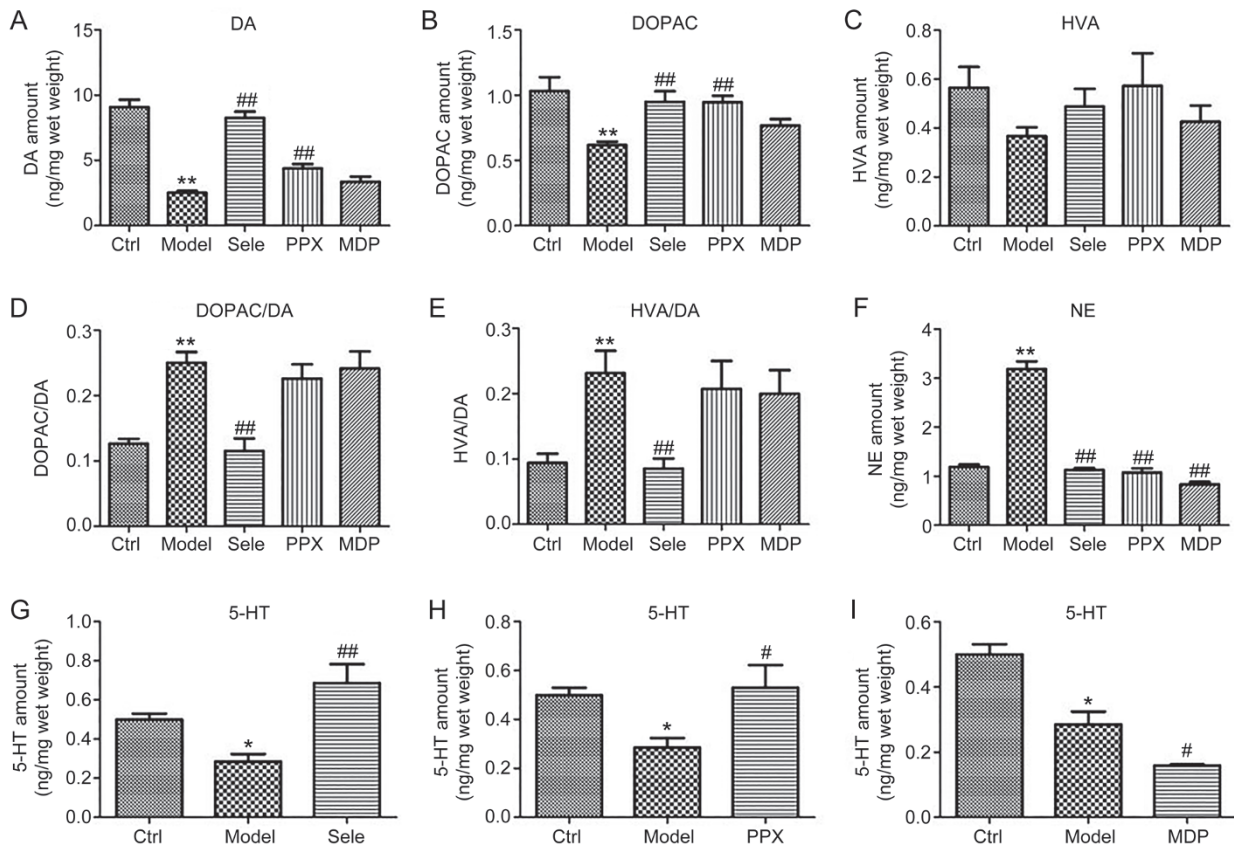


**Figure 2.** Effects of selegiline, pramipexole and medopar on neurotransmitters in the striatum region. Data are presented as the mean±SEM.  $n=5-7$ . One-way ANOVA test followed by Duncan's test. \* $P<0.05$ , \*\* $P<0.01$  vs the control group. # $P<0.05$ , ## $P<0.01$  vs the model group.

cell bodies with thickened electron density and swollen organelle structures (Figure 6g). Both selegiline (Figure 6c, 6h) and pramipexole (Figure 6d, 6i) showed a protective effect against the damage of both myelin sheaths and neurons in the spinal cord, but medopar (Figure 6e, 6j) appeared to not have an effect.

## Discussion

First and foremost, we discuss the motor performance after subacute MPTP treatment. Up until now, the behavioral assessments in the subacute MPTP mouse model are still controversial. Many studies have described motor defects<sup>[12-14]</sup>, while others have proven that the model hardly mimics the movement disorder of PD and may even induce hyperactivity in animals<sup>[10, 15, 16]</sup>. Here, in our research, subacute MPTP treatment failed to cause typical movement defects in spite of the serious damage to the dopaminergic neurons and the remarkable decrease in DA content. Instead of a motor deficit, the results of the rotarod test in our study demonstrated that MPTP-treated mice could walk on the rotarod longer than controls. The longer latency for the model animals in the rotarod test, in fact, is not deemed as a normal performance, and this kind of behavioral hyperactivity is likely to be caused by the evident increase in NE content<sup>[17-19]</sup>. NE, similar to DA, also plays a key role in animal behavior<sup>[17-19]</sup>. A study showed

that NE depletion after lesions of the locus coeruleus (LC), the major noradrenergic nucleus in the brain, could potentiate MPTP toxicity<sup>[20]</sup>. In addition, Rommelfanger *et al* found that NE loss could induce more profound motor defects than the DA loss induced by MPTP treatment<sup>[17]</sup>. Clinically, lesion of the NE system is also involved in PD progression, but the MPTP model failed to cause an LC lesion<sup>[20, 21]</sup>. Therefore, NE deficiency may be a further requirement for motor impairment<sup>[18]</sup>.

Apart from the NE system, the DA system has its own compensatory ability, such as the supplementary induction of TH synthesis and the increased responsiveness of striatal neurons to DA<sup>[16]</sup>. In addition, DA turnover also plays an important part in the compensatory preservation of dopaminergic function for behavioral ability<sup>[15, 16]</sup>. In our research, we indeed found that the DA metabolite ratios (DOPAC/DA and HVA/DA, indexes for DA turnover) increased significantly, which further accounted for the failure of the behavioral deficits after MPTP treatment. In conclusion, the nigrostriatal system has a strong compensatory ability for DA loss (Figure 7A). Though the DA content was exhausted, the NE level and the DA metabolite ratios were compensatively increased to regulate the unbalanced nigrostriatal system. These results could account for why the model mice did not behave abnormally and even gained hyperactivity. When DA depletion is more

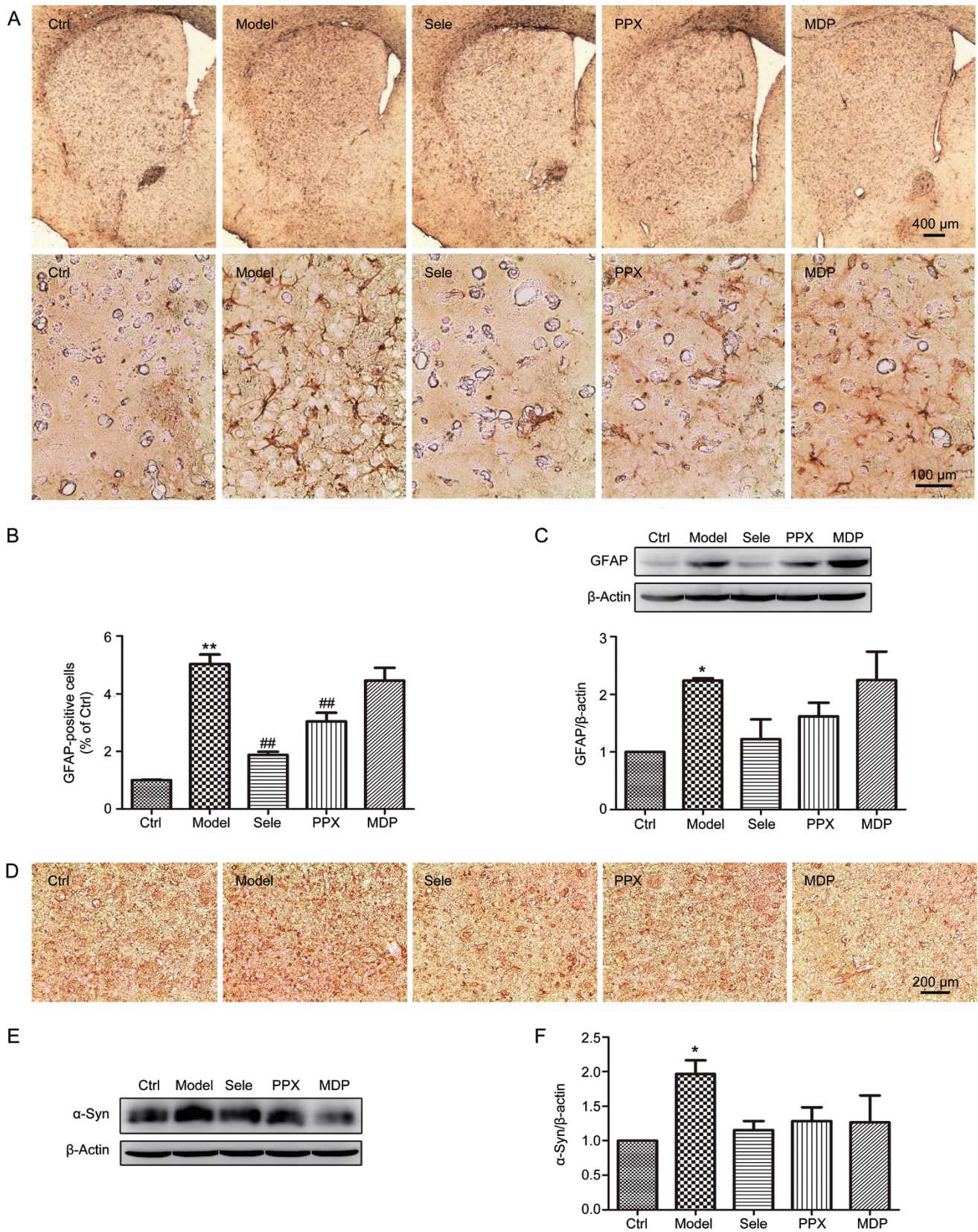


**Figure 3.** Effects of selegiline, pramipexole and medopar on astrocytes and  $\alpha$ -synuclein in the striatum region. (A) Immunohistochemical staining of GFAP<sup>+</sup> cells. (B) Quantitative analysis of GFAP<sup>+</sup> cells. (C) Western blot assay of GFAP in the striatum region. (D) Immunohistochemical staining of  $\alpha$ -synuclein. (E, F) Western blot assay of  $\alpha$ -synuclein content in striatum tissue. Data are presented as the mean  $\pm$  SEM.  $n=3$ . One-way ANOVA test followed by Duncan's test. \* $P<0.05$ , \*\* $P<0.01$  vs the control group. ## $P<0.01$  vs the model group.



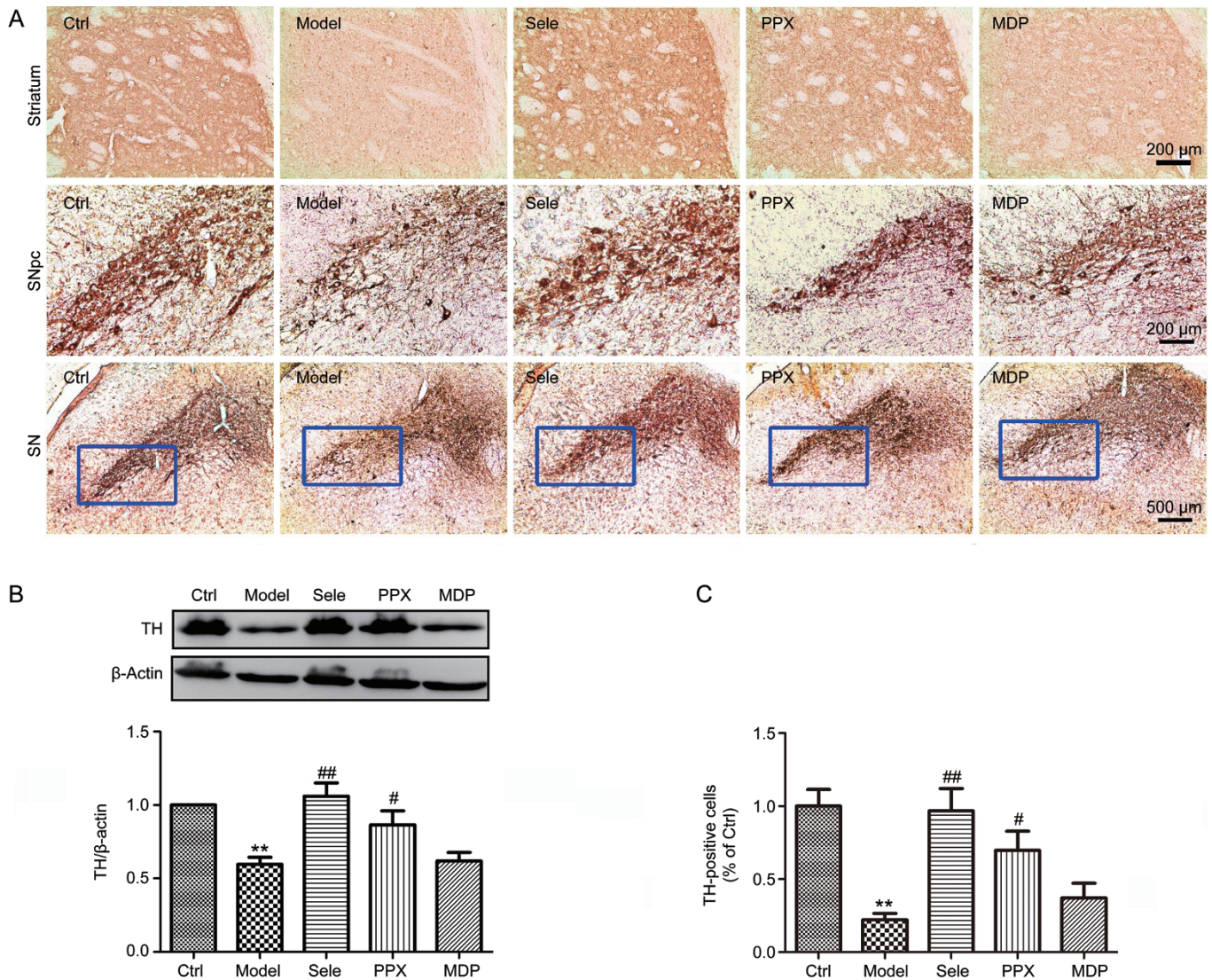


**Figure 4.** Effects of selegiline, pramipexole and medopar on dopaminergic terminals in the striatum and cells in the SNpc. (A) Immunohistochemical staining of TH in the nigrostriatal system. (B) Western blot assay of TH content in striatum tissue.  $n=5$ . (C) Quantitative analysis of TH<sup>+</sup> cells in the SNpc region.  $n=3$ . Data are presented as the mean±SEM. One-way ANOVA test followed by Duncan's test. \*\* $P<0.01$  vs the control group. # $P<0.05$ , ## $P<0.01$  vs the model group.

than 80%<sup>[16]</sup>, the destruction is too severe to be compensated, resulting in movement disability (Figure 7A). That is, the current subacute MPTP model in this study is not enough to cause motor disability, but assessing the damage in the dopaminergic system is still valuable. Moreover, to overcome this limitation, the chronic MPTP model may be considered as we have previously confirmed dyskinesia in chronic MPTP-treated mice<sup>[11]</sup>. In addition, we can also try to destroy the NE system to induce motor disability in MPTP-treated mice<sup>[17]</sup>.

Next, we will discuss the abnormal changes induced by the subacute MPTP treatment. Many pathological changes in this model, such as the increase in  $\alpha$ -synuclein, astrocyte activation and BBB destruction, are all associated with the development of PD<sup>[22-24]</sup>. These changes can affect one another to form a vicious circle, driving the degeneration of the nigrostriatal

system (Figure 7B). On the one hand, the unusual increased  $\alpha$ -synuclein may enhance its own toxicity by modification or aggregation of itself and then activate glial cells to induce inflammation and oxidative stress, which in turn promote aberrant  $\alpha$ -synuclein formation<sup>[25, 26]</sup>. Moreover,  $\alpha$ -synuclein may be transferred from axon terminals to astrocytes and form  $\alpha$ -synuclein inclusions similar to LBs. On the other hand, both the inflammation induced by  $\alpha$ -synuclein and the central immune response mediated by astrocytes and microglial cells would destroy the integrity of the BBB<sup>[27]</sup>, and in turn the BBB lesion would recruit peripheral immune cells by increasing the infiltration of CD4<sup>+</sup> and CD8<sup>+</sup> T lymphocytes<sup>[28, 29]</sup>. The complex relationships among  $\alpha$ -synuclein dysfunction, astrocyte activation and BBB destruction are responsible for accelerating PD degeneration (Figure 7B). In our research, MPTP led to



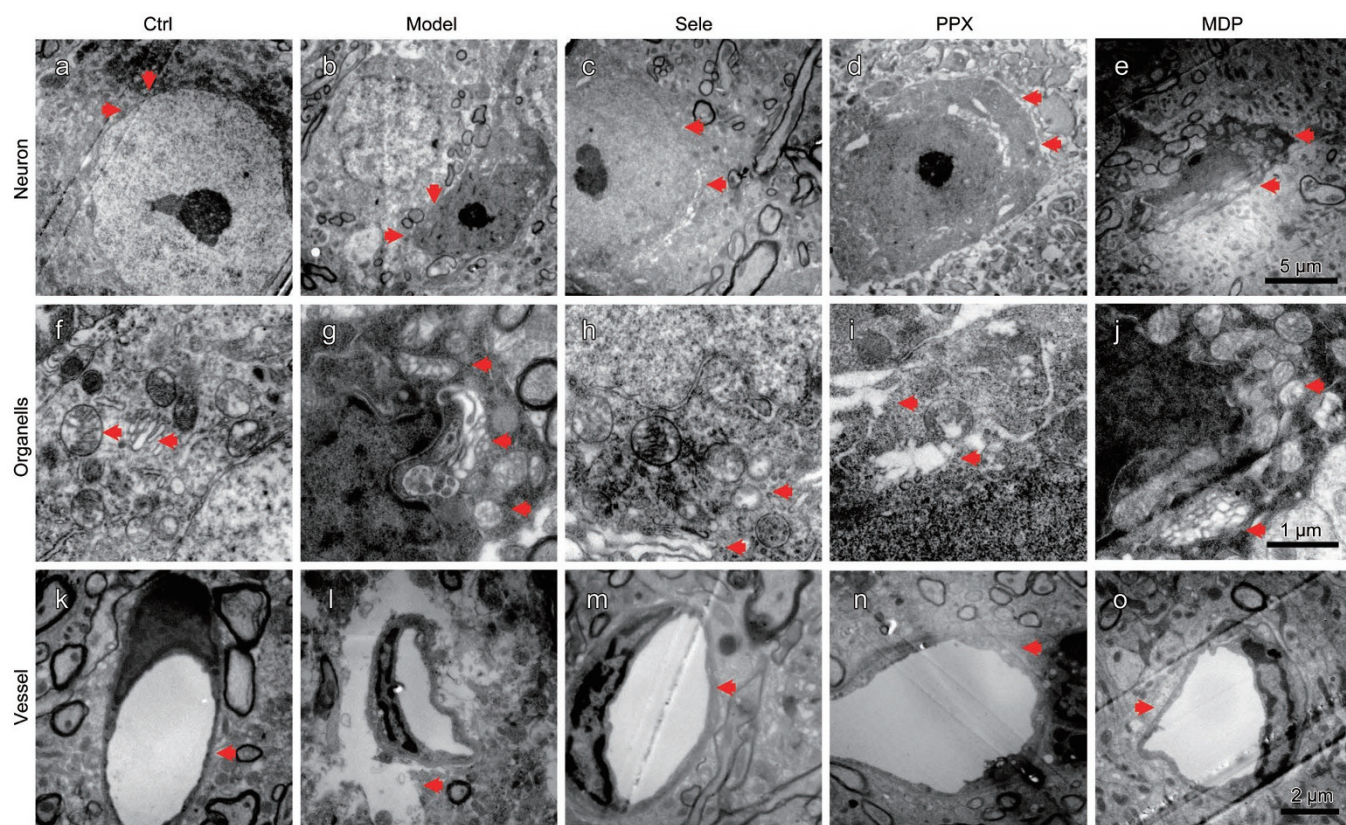


**Figure 5.** Effects of selegiline (Sele), pramipexole (PPX) and medopar (MDP) on ultrastructure destruction in the SNpc region. As shown by red arrows, the TEM images of the control brain region showed an intact structure of the cell bodies (a), organelles (f) and BBB (k), while the model neuron was severely damaged exhibiting heavy electron density and swollen mitochondria, Golgi apparatus and BBB (b, g, l). Both selegiline (c, h, m) and pramipexole (d, i, n) had protective functions against the MPTP-induced damage. The protective role of medopar was not displayed in terms of cell morphology (e) and organelle structure (j).

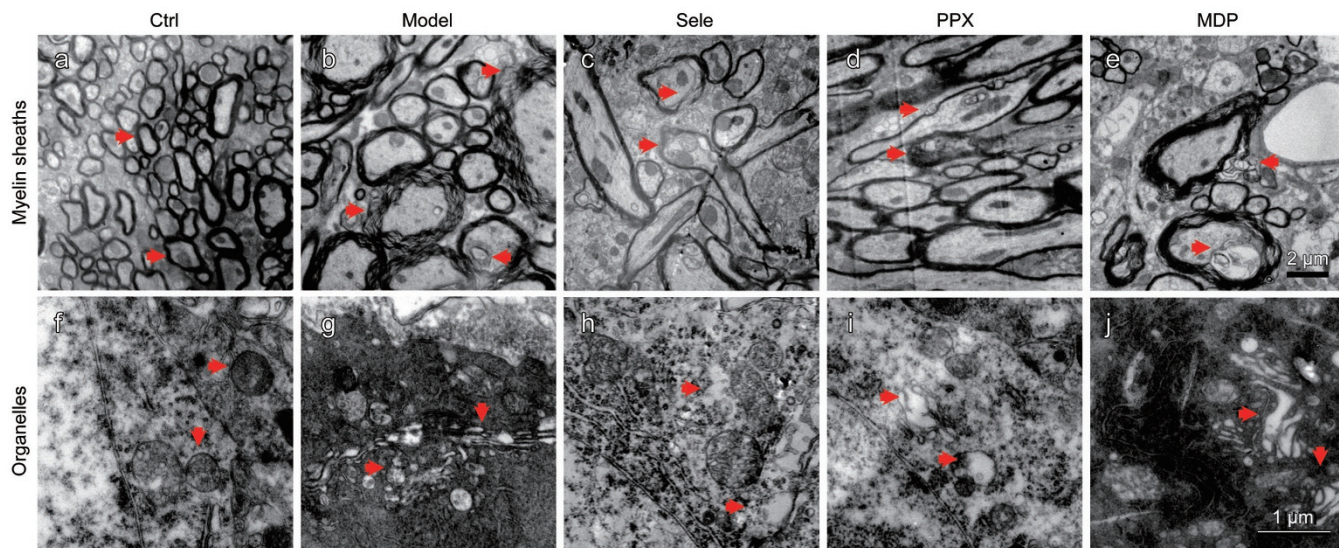


**Figure 6.** Effects of selegiline (Sele), pramipexole (PPX) and medopar (MDP) on ultrastructure destruction in the spinal cord. As shown by red arrows, the myelin sheaths of the control (a) are well organized, while the model myelin sheaths (b) are discrete and loose. Selegiline (c) and pramipexole (d) but not medopar (e) play protective roles. The organelles such as mitochondria and the Golgi apparatus are normal in control neurons in the spinal cord (f), while that in the MPTP-treated mice have a damaged structure (g). Selegiline (h) and pramipexole (i) but not medopar (j) show improving effects.



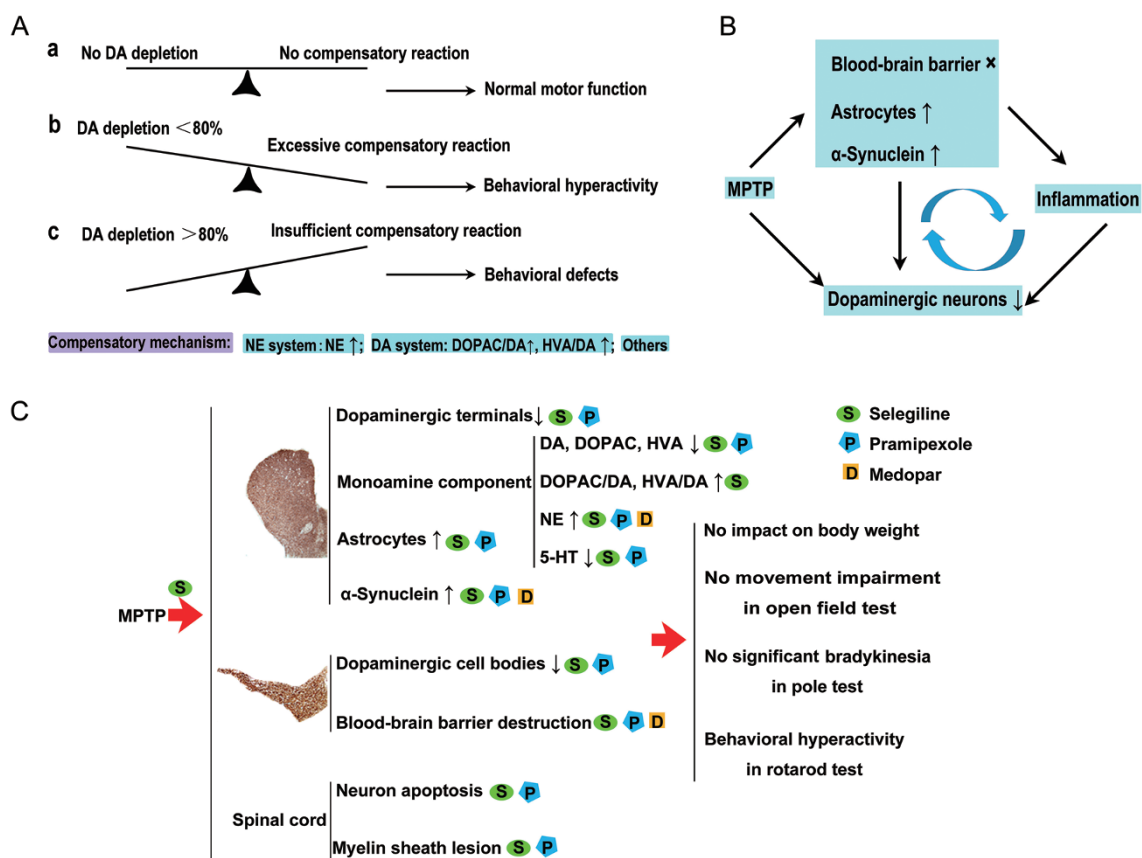


**Figure 7.** The summary scheme. (A) The balance between DA depletion and a compensatory reaction: (a) normal motor function; (b) behavioral hyperactivity induced by an excessive compensatory reaction; (c) behavioral defects induced by severe DA depletion. (B) The abnormal changes induced by the subacute MPTP treatment. (C) Effects of selegiline, pramipexole and medopar on the MPTP-induced damages in the striatum, the SNpc and the spinal cord.

a significant increase in  $\alpha$ -synuclein, an evident activation of astrocytes and a severe destruction of the BBB. These changes would play key roles in Parkinsonian degeneration and, thus, should be taken into consideration in the study of PD pathogenesis.

Moreover, motor neuron loss in the spinal cord has been reported in MPTP models<sup>[30, 31]</sup> as well as PD patients<sup>[32]</sup>. Our experiment also demonstrated injured neurons in the spinal cord characterized by nuclear condensation and organelle vacuolation. In addition, we found a disordered, discrete myelin structure in the spinal cord irritated by MPTP. Myelin sheaths are generated throughout life with a multilamellar membrane structure by the wrapping and compaction of oligodendrocytes<sup>[33]</sup>. The function of the myelin sheaths is mainly to ensure fast and efficient electrical signal transduction through nerve fibers<sup>[34]</sup>. As reported previously, myelin dysfunction has been commonly observed in multiple system atrophy (MSA)<sup>[35]</sup>, and  $\alpha$ -synuclein may be involved in the myelin deficit<sup>[36]</sup>. In this study, the loose myelin structure induced by MPTP indicates a possible relationship between PD degeneration and  $\alpha$ -synuclein-induced myelin damage.

Last but not least, we will discuss the effects of selegiline, pramipexole, and medopar on the subacute MPTP mouse

model (Figure 7C). The curative effects of these drugs on clinical treatment and animal evaluation seem varied, but actually, they are not contradictory. The reasons are stated as follows.

Selegiline can maintain the DA levels in the striatum by inhibiting the metabolism of DA and can also, as an antioxidant, clean the radicals produced by oxidative stress. Clinically, selegiline is known to be well tolerated but less effective than either *L*-dopa or pramipexole in motor improvement and has been proposed as a disease-modifying agent, for it seems to delay the disease progression<sup>[4]</sup>. However, in our study, selegiline played a stronger protective role in MPTP-treated mice than medopar and pramipexole and actually protected the striatum, the SNpc, and the spinal cord from MPTP to nearly a normal status (Figure 7C). This is because selegiline is a specific inhibitor of monoamine oxidase B and can prevent MPTP from being converted into its metabolite MPP<sup>+</sup>, which is toxic to neurons. Although selegiline shows varied degrees of protection on experimental animals and clinical patients and the MPP<sup>+</sup> amount exposed to neurons is affected by selegiline, there are two reasons to include selegiline in the experimental design. First, we can use selegiline as a positive control to validate the pathological changes induced by MPTP. Additionally, we can use selegiline to test anti-PD candidates that

are also classified as MAO-B inhibitors, for these types of candidates may be able to be developed into anti-PD drugs.

Pramipexole, as a non-ergoline dopamine receptor agonist, is also a common first-line medication and does not trigger dyskinesias. However, side effects exist, such as early gastrointestinal or psychiatric disorders, ankle oedema, and sleep attacks<sup>[4]</sup>. Pramipexole (PPX) can efficiently relieve the clinical motor disturbances by selectively exciting dopamine D<sub>3</sub> receptors. However, beyond the dopamine receptor interactions, other protective mechanism also exist<sup>[37]</sup>, such as its antioxidant properties, apoptotic pathway inhibition, mitochondrial membrane stabilization, and cytotrophic effects<sup>[38–40]</sup>. In agreement with the above studies, our work showed that pramipexole prevented the MPTP damage of the nigrostriatal dopaminergic neurons and then attenuated the loss of DA (Figure 7C). Furthermore, in this study, pramipexole had a wide protection on the 5-HT level, astrocytes, BBB, and myelin sheath (Figure 7C).

Clinically, *L*-dopa combined with benserazide or carbidopa is the most popular therapy to efficiently improve behavioral symptoms<sup>[4]</sup>. However, long-term treatment induces severe adverse effects. Despite the overt behavioral improvement, whether *L*-dopa is protective or toxic to dopaminergic neurons remains debatable. Some researchers have attributed its protective effects to its neurotrophic properties<sup>[39, 41, 42]</sup>, while others have confirmed its toxicity by inducing oxidative stress and inflammation<sup>[43–45]</sup>. In our research, medopar, a combination of *L*-dopa and benserazide, was unable to protect the striatum, the SNpc, and the spinal cord from MPTP injury (Figure 7C). In fact, the abundant increase in DA from medopar treatment did not increase the endogenous DA production<sup>[46]</sup> and eliminated the compensatory increase in NE (Figure 7C). In addition, we found that medopar suppressed the striatal 5-HT production (Figure 7C), indicating the presence of lesions of serotonergic neurons caused by *L*-dopa<sup>[47, 48]</sup>.

All in all, we make the following conclusions. First, the subacute MPTP treatment was successful at destroying the dopaminergic neurons, resulting in a reduced secretion of DA in the striatum. However, the NE system and DA system had a compensatory response, leading to the failure to trigger a movement disability and perhaps even causing hyperactivity of the mice. Despite this compensation, the subacute MPTP model is still valuable for assessing the effect of candidate drugs on the nigrostriatal pathway, which is damaged before the emergence of a motor disability. Second, MPTP increased the  $\alpha$ -synuclein protein level, activated astrocytes, and destroyed the BBB structure. In addition, these clinically relevant targets ( $\alpha$ -synuclein, astrocyte, and BBB) are worthy to be studied further in research on the pathogenesis of PD and the efficacy of treatment. Third, both selegiline and pramipexole improved the injuries caused by MPTP treatment, while medopar did not show a protective function. Therefore, selegiline or pramipexole is suggested to be used as a positive control in the MPTP model to assess therapeutic candidates. However, from the perspective of pathology, medopar is not suitable to be selected as a positive control.

## Acknowledgements

This work was supported by the National Natural Science Foundation of China (No 81373997, U1402221, 81573640, 81603316), Beijing Natural Science Foundation (No 7161011), the Beijing Key Laboratory of New Drug Mechanisms and Pharmacological Evaluation Study (No BZ0150), CAMS Innovation Fund for Medical Sciences (CIFMS) (No 2016-I2M-1-004), Key Research and Development Project of Hunan Province (No 2015SK2029-1), and the Scientific Research Foundation of the Higher Education Institutions of Hunan Province (No 15K091).

## Author contribution

Yu-he YUAN, Nai-hong CHEN, and Qiu-shuang ZHANG designed the study; Qiu-shuang ZHANG performed the experiments and did the data analysis; Yang HENG, Zheng MOU, and Ju-yang HUANG contributed to the tissue preparation; Zheng MOU helped conduct the HPLC analysis.

## Abbreviations

5-HT, serotonin; BBB, blood-brain barrier; Ctrl, control; DA, dopamine; DOPAC, dihydroxy-phenyl acetic acid; GFAP, glial fibrillary acidic protein; HPLC, high-performance liquid chromatography; HVA, homovanillic acid; LBs, Lewy bodies; LC, locus coeruleus; MAO-B, monoamine oxidase B; MDP, medopar; MPP<sup>+</sup>, 1-methyl-4-phenylpyridinium ion; MPTP, 1-methyl-4-phenyl-1,2,3,6-tetrahydropyridine; MSA, multiple system atrophy; NE, norepinephrine; PD, Parkinson's disease; PPX, pramipexole; Sele, selegiline; SN, substantia nigra; SNpc, substantia nigra pars compacta; TEM, transmission electron microscope; TH, tyrosine hydroxylase.

## References

- 1 Connolly BS, Lang AE. Pharmacological treatment of Parkinson disease: a review. *JAMA* 2014; 311: 1670–83.
- 2 Giugni JC, Okun MS. Treatment of advanced Parkinson's disease. *Curr Opin Neurol* 2014; 27: 450–60.
- 3 Dauer W, Przedborski S. Parkinson's disease: mechanisms and models. *Neuron* 2003; 39: 889–909.
- 4 Lees AJ, Hardy J, Revesz T. Parkinson's disease. *Lancet* 2009; 373: 2055–66.
- 5 Blandini F, Armentero MT. Animal models of Parkinson's disease. *FEBS J* 2012; 279: 1156–66.
- 6 Petroske E, Meredith GE, Callen S, Totterdell S, Lau YS. Mouse model of Parkinsonism: a comparison between subacute MPTP and chronic MPTP/probenecid treatment. *Neuroscience* 2001; 106: 589–601.
- 7 Ren Z, Yang N, Ji C, Zheng J, Wang T, Liu Y, et al. Neuroprotective effects of 5-(4-hydroxy-3-dimethoxybenzylidene)-thiazolidinone in MPTP induced Parkinsonism model in mice. *Neuropharmacology* 2015; 93: 209–18.
- 8 Xiao-Feng L, Wen-Ting Z, Yuan-Yuan X, Chong-Fa L, Lu Z, Jin-Jun R, et al. Protective role of 6-hydroxy-1-H-indazole in an MPTP-induced mouse model of Parkinson's disease. *Eur J Pharmacol* 2016; 791: 348–54.
- 9 Selvakumar GP, Janakiraman U, Essa MM, Justin Thenmozhi A, Manivasagam T. Escin attenuates behavioral impairments, oxidative stress and inflammation in a chronic MPTP/probenecid mouse model of Parkinson's disease. *Brain Res* 2014; 1585: 23–36.

- 10 Luchtman DW, Shao D, Song C. Behavior, neurotransmitters and inflammation in three regimens of the MPTP mouse model of Parkinson's disease. *Physiol Behavior* 2009; 98: 130–8.
- 11 Heng Y, Zhang QS, Mu Z, Hu JF, Yuan YH, Chen NH. Ginsenoside Rg1 attenuates motor impairment and neuroinflammation in the MPTP-probenecid-induced parkinsonism mouse model by targeting alpha-synuclein abnormalities in the substantia nigra. *Toxicol Lett* 2016; 243: 7–21.
- 12 Li XH, Dai CF, Chen L, Zhou WT, Han HL, Dong ZF. 7,8-Dihydroxyflavone ameliorates motor deficits via suppressing alpha-synuclein expression and oxidative stress in the MPTP-induced mouse model of Parkinson's disease. *CNS Neurosci Ther* 2016; 22: 617–24.
- 13 Ji C, Xue GF, Lijun C, Feng P, Li D, Li L, et al. A novel dual GLP-1 and GIP receptor agonist is neuroprotective in the MPTP mouse model of Parkinson's disease by increasing expression of BDNF. *Brain Res* 2016; 1634: 1–11.
- 14 Sim Y, Park G, Eo H, Huh E, Gu PS, Hong SP, et al. Protective effects of a herbal extract combination of *Bupleurum falcatum*, *Paeonia suffruticosa*, and *Angelica dahurica* against MPTP-induced neurotoxicity via regulation of nuclear receptor-related 1 protein. *Neuroscience* 2016; 340: 166–75.
- 15 Rousset E, Joubert C, Callebert J, Parain K, Tremblay L, Orioux G, et al. Behavioral changes are not directly related to striatal monoamine levels, number of nigral neurons, or dose of parkinsonian toxin MPTP in mice. *Neurobiol Dis* 2003; 14: 218–28.
- 16 Bezaud E, Gross CE. Compensatory mechanisms in experimental and human parkinsonism: towards a dynamic approach. *Prog Neurobiol* 1998; 55: 93–116.
- 17 Rommelfanger KS, Edwards GL, Freeman KG, Liles LC, Miller GW, Weinshenker D. Norepinephrine loss produces more profound motor deficits than MPTP treatment in mice. *Proc Natl Acad Sci U S A* 2007; 104: 13804–9.
- 18 Rommelfanger KS, Weinshenker D. Norepinephrine: the redheaded stepchild of Parkinson's disease. *Biochem Pharmacol* 2007; 74: 177–90.
- 19 Brichta L, Greengard P, Flajolet M. Advances in the pharmacological treatment of Parkinson's disease: targeting neurotransmitter systems. *Trends Neurosci* 2013; 36: 543–54.
- 20 Yao N, Wu Y, Zhou Y, Ju L, Liu Y, Ju R, et al. Lesion of the locus coeruleus aggravates dopaminergic neuron degeneration by modulating microglial function in mouse models of Parkinson's disease. *Brain Res* 2015; 1625: 255–74.
- 21 Marien MR, Colpaert FC, Rosenquist AC. Noradrenergic mechanisms in neurodegenerative diseases: a theory. *Brain Res Brain Res Rev* 2004; 45: 38–78.
- 22 Desai BS, Monahan AJ, Carvey PM, Hendey B. Blood-brain barrier pathology in Alzheimer's and Parkinson's disease: implications for drug therapy. *Cell Transplant* 2007; 16: 285–99.
- 23 Kortekaas R, Leenders KL, van Oostrom JC, Vaalburg W, Bart J, Willemsen AT, et al. Blood-brain barrier dysfunction in parkinsonian midbrain *in vivo*. *Ann Neurol* 2005; 57: 176–9.
- 24 Pisani V, Stefani A, Pierantozzi M, Natoli S, Stanzione P, Franciotta D, et al. Increased blood-cerebrospinal fluid transfer of albumin in advanced Parkinson's disease. *J Neuroinflammation* 2012; 9: 188.
- 25 Halliday GM, Stevens CH. Glia: initiators and progressors of pathology in Parkinson's disease. *Movement Disorders* 2011; 26: 6–17.
- 26 Zhang QS, Heng Y, Yuan YH, Chen NH. Pathological alpha-synuclein exacerbates the progression of Parkinson's disease through microglial activation. *Toxicol Lett* 2017; 265: 30–7.
- 27 Reale M, Iarlori C, Thomas A, Gambi D, Perfetti B, Di Nicola M, et al. Peripheral cytokines profile in Parkinson's disease. *Brain Behavior Immunity* 2009; 23: 55–63.
- 28 Brochard V, Combadiere B, Prigent A, Laouar Y, Perrin A, Beray-Berthet V, et al. Infiltration of CD4<sup>+</sup> lymphocytes into the brain contributes to neurodegeneration in a mouse model of Parkinson disease. *J Clin Invest* 2009; 119: 182–92.
- 29 Depboylu C, Stricker S, Ghobril JP, Oertel WH, Priller J, Höglinger GU. Brain-resident microglia predominate over infiltrating myeloid cells in activation, phagocytosis and interaction with T-lymphocytes in the MPTP mouse model of Parkinson disease. *Exp Neurol* 2012; 238: 183–91.
- 30 Samantaray S, Knaryan VH, Butler JT, Ray SK, Banik NL. Spinal cord degeneration in C57BL/6N mice following induction of experimental parkinsonism with MPTP. *J Neurochem* 2008; 104: 1309–20.
- 31 Vivacqua G, Biagioni F, Yu S, Casini A, Bucci D, D'Este L, et al. Loss of spinal motor neurons and alteration of alpha-synuclein immunostaining in MPTP induced Parkinsonism in mice. *J Chem Neuroanat* 2012; 44: 76–85.
- 32 Samantaray S, Knaryan VH, Shields DC, Banik NL. Critical role of calpain in spinal cord degeneration in Parkinson's disease. *J Neurochem* 2013; 127: 880–90.
- 33 Young KM, Psachoulia K, Tripathi RB, Dunn SJ, Cossell L, Attwell D, et al. Oligodendrocyte dynamics in the healthy adult CNS: evidence for myelin remodeling. *Neuron* 2013; 77: 873–85.
- 34 Simons M, Nave KA. Oligodendrocytes: myelination and axonal support. *Cold Spring Harbor Perspec Biol* 2016; 8: a020479.
- 35 Wong JH, Halliday GM, Kim WS. Exploring myelin dysfunction in multiple system atrophy. *Exp Neurobiol* 2014; 23: 337–44.
- 36 Ettle B, Kerman BE, Valera E, Gillmann C, Schlachetzki JC, Reiprich S, et al. Alpha-synuclein-induced myelination deficit defines a novel interventional target for multiple system atrophy. *Acta Neuropathol* 2016; 132: 59–75.
- 37 Ramirez AD, Wong SK, Menniti FS. Pramipexole inhibits MPTP toxicity in mice by dopamine D3 receptor dependent and independent mechanisms. *Eur J Pharmacol* 2003; 475: 29–35.
- 38 Iida M, Miyazaki I, Tanaka K, Kabuto H, Iwata-Ichikawa E, Ogawa N. Dopamine D<sub>2</sub> receptor-mediated antioxidant and neuroprotective effects of ropinirole, a dopamine agonist. *Brain Res* 1999; 838: 51–9.
- 39 Shin JY, Park HJ, Ahn YH, Lee PH. Neuroprotective effect of L-dopa on dopaminergic neurons is comparable to pramipexol in MPTP-treated animal model of Parkinson's disease: a direct comparison study. *J Neurochem* 2009; 111: 1042–50.
- 40 Gu M, Iravani MM, Cooper JM, King D, Jenner P, Schapira AH. Pramipexole protects against apoptotic cell death by non-dopaminergic mechanisms. *J Neurochem* 2004; 91: 1075–81.
- 41 Guo Z, Xu S, Du N, Liu J, Huang Y, Han M. Neuroprotective effects of stemazole in the MPTP-induced acute model of Parkinson's disease: Involvement of the dopamine system. *Neurosci Lett* 2016; 616: 152–9.
- 42 Mena MA, Davila V, Bogaluvsky J, Sulzer D. A synergistic neurotrophic response to l-dihydroxyphenylalanine and nerve growth factor. *Mol Pharmacol* 1998; 54: 678–86.
- 43 Blunt SB, Jenner P, Marsden CD. Suppressive effect of L-dopa on dopamine cells remaining in the ventral tegmental area of rats previously exposed to the neurotoxin 6-hydroxydopamine. *Mov Disord* 1993; 8: 129–33.
- 44 Segura-Aguilar J, Paris I, Munoz P, Ferrari E, Zecca L, Zucca FA. Protective and toxic roles of dopamine in Parkinson's disease. *J Neurochem* 2014; 129: 898–915.
- 45 Carta AR, Mulas G, Bortolanza M, Duarte T, Pillai E, Fisone G, et al. L-DOPA-induced dyskinesia and neuroinflammation: do microglia and

- astrocytes play a role? *Eur J Neurosci* 2017; 45: 73–91.
- 46 Porras G, De Deurwaerdere P, Li Q, Marti M, Morgenstern R, Sohr R, et al. *L*-dopa-induced dyskinesia: beyond an excessive dopamine tone in the striatum. *Sci Rep* 2014; 4: 3730.
- 47 Navailles S, Bioulac B, Gross C, De Deurwaerdere P. Chronic *L*-DOPA therapy alters central serotonergic function and *L*-DOPA-induced dopamine release in a region-dependent manner in a rat model of Parkinson's disease. *Neurobiol Dis* 2011; 41: 585–90.
- 48 Borah A, Mohanakumar KP. Long-term *L*-DOPA treatment causes indiscriminate increase in dopamine levels at the cost of serotonin synthesis in discrete brain regions of rats. *Cell Mol Neurobiol* 2007; 27: 985–96.